Mechanical Systems and Signal Processing 75 (2016) 41–56

Contents lists available at ScienceDirect

Mechanical Systems and Signal Processing

journal homepage: www.elsevier.com/locate/ymssp

Polynomial chaos expansion with random and fuzzy variables

E. Jacquelin [a,b,c,*], M.I. Friswell [d], S. Adhikari [d], O. Dessombz [e], J.-J. Sinou [e,f]

[a] Université de Lyon, F-69622 Lyon, France
[b] Université Claude Bernard Lyon 1, Villeurbanne
[c] IFSTTAR, UMR-T9406, LBMC Laboratoire de Biomécanique et Mécanique des chocs, F69675 Bron
[d] College of Engineering, Swansea University, Swansea SA2 8PP, UK
[e] École Centrale de Lyon, LTDS Laboratoire de Tribologie et Dynamique des Systèmes UMR CNRS 5513, F-69134 Écully, France
[f] Institut Universitaire de France, 75005 Paris, France

ARTICLE INFO

Article history:
Received 28 July 2015
Received in revised form
9 November 2015
Accepted 5 December 2015
Available online 21 December 2015

Keywords:
Random systems
Structural dynamics
Polynomial chaos expansion
Fuzzy variables
Random variables
Steady-state response

ABSTRACT

A dynamical uncertain system is studied in this paper. Two kinds of uncertainties are addressed, where the uncertain parameters are described through random variables and/or fuzzy variables. A general framework is proposed to deal with both kinds of uncertainty using a polynomial chaos expansion (PCE). It is shown that fuzzy variables may be expanded in terms of polynomial chaos when Legendre polynomials are used. The components of the PCE are a solution of an equation that does not depend on the nature of uncertainty. Once this equation is solved, the post-processing of the data gives the moments of the random response when the uncertainties are random or gives the response interval when the variables are fuzzy. With the PCE approach, it is also possible to deal with mixed uncertainty, when some parameters are random and others are fuzzy. The results provide a fuzzy description of the response statistical moments.

1. Introduction

The design of vibrating structures requires an appropriate model that is often transformed to a finite element model for computation. However parameters of the model may be uncertain, and the first issue is to describe uncertainties. Some parameters may be described through a probabilistic description whereas insufficient information can be gathered for some others. The latter parameters can be modeled by fuzzy parameters [1,2], when the possible domain of variation is known; this approach has been successfully applied to determine the frequency response functions of uncertain dynamical systems [3–5]. The probabilistic approach is appealing but the statistical law is sometimes difficult to estimate. So, in practice, the laws are often supposed to follow a normal, log-normal or uniform distribution. For reliable estimate of probability distribution functions, significant amount if data is necessary. In the absence of large data, imprecise probability approaches can be used [6]. In this paper, we consider that some variables are described probabilistically while some variables are described by a fuzzy approach.

The second issue is the propagation of the uncertainties, that is to describe the responses when the parameters vary. Monte Carlo simulation (MCS) is probably the oldest method used to study uncertainty propagation. The expansion-based methods [7–10], such as the spectral approaches, are alternatives to MCS. Polynomial chaos (PC) expansion (PCE) using a

* Corresponding author at: Université de Lyon, F-69622 Lyon, France. Tel.: +33 478931671.
E-mail addresses: eric.jacquelin@univ-lyon1.fr (E. Jacquelin), M.I.Friswell@swansea.ac.uk (M.I. Friswell), S.Adhikari@swansea.ac.uk (S. Adhikari), olivier.dessombz@ec-lyon.fr (O. Dessombz), Jean-Jacques.Sinou@ec-lyon.fr (J.-J. Sinou).

http://dx.doi.org/10.1016/j.ymssp.2015.12.001
0888-3270/

Galerkin scheme is one of the most widely used spectral methods. Hermite polynomials are the most used even if other orthogonal polynomials may be successfully used [11,12]. For instance, Legendre polynomials are used to propagate uniform random uncertainties. Sudret et al. made the PCE technique possible for a large number of uncertain parameters, by using an adaptive sparse PCE [13,14].

The PC method has been already applied to calculate the response of an uncertain dynamical system with fuzzy variables [15,16]. This approach requires the use of Legendre polynomials. Monti et al. used a similar approach to extend PCE to interval analysis [17].

The main objective of this paper is to give a general framework to derive the response of an uncertain linear dynamical system in terms of a PCE; the uncertainty may be described either by random variables or by fuzzy variables or by mixed uncertain variables (random and fuzzy). First background on the PCE and on fuzzy variables is given. Second, the equation satisfied by the PC component is derived. Finally examples with two uncertain parameters are studied to illustrate the method.

2. Finite element analysis with uncertain systems

The response to a dynamic excitation is modeled by a finite element approximation, where the inertia, damping and stiffness properties are assumed to be uncertain. The global matrices (mass, damping and stiffness) are obtained by the assembly procedure and the response is governed by

$$\mathbf{M}\ddot{\mathbf{x}}(t)+\mathbf{D}\dot{\mathbf{x}}(t)+\mathbf{K}\mathbf{x}(t)=\mathbf{F}(t) \tag{1}$$

where $\mathbf{M}$, $\mathbf{D}$ and $\mathbf{K}$ are the uncertain mass, damping and stiffness matrices, $\mathbf{x}(t)$ is the vector of generalized co-ordinates and $\mathbf{F}$ is the excitation vector. Matrices $\mathbf{M}$, $\mathbf{D}$ and $\mathbf{K}$ depend on the uncertain parameters, which are either fuzzy variables or random variables. The random variables are described by the associated probability density function (pdf).

For notational convenience let $\mathbf{A}$ denote an uncertain matrix that may be $\mathbf{M}$, $\mathbf{D}$ or $\mathbf{K}$. In the next subsections $\mathbf{A}$ will be given for both cases of uncertainty, with $\mathbf{A}$ assumed to be given by the expansion

$$\mathbf{A}=\mathbf{A}(\mathcal{A})=\mathbf{A}_0+\sum_{i=1}^{r} a_i\mathbf{A}_i \tag{2}$$

where $\mathcal{A}=(a_1,\ldots,a_r)$ gathers all the uncertain parameters a_i.

2.1. Random variables

$\mathbf{A}$ is a random matrix and then uncertainties are associated with probability density functions (pdfs). Expression (2) may represent a Karhunen–Loève expansion. $\mathcal{A}=(a_1,\ldots,a_r)$ is a random vector, where a_i is a random variable with zero-mean and $\mathbf{A}_0$ is the mean matrix. However, as mentioned by Stefanou [9], the pdf of the random variables is provided by experimental measurements and often the lack of data forces assumptions to be made. Recently, Sepahvand and Marburg [18,19] proposed a new method to estimate these pdfs from vibration tests, by using the Pearson model and a generalized polynomial chaos expansion. Gaussian random variables are often chosen as a result of theoretical justification (central limit theorem, maximum entropy when the first two moments are known) and also for its simplicity. However, other distribution may be used, such as the uniform distribution, which will be used in the examples given in Section 4.

The ultimate objective of the propagation of uncertainties is to derive the pdf of the random vector $\mathbf{x}(t)$. In this paper, the first two moments of the response will be estimated for each time t in the time domain, or for each frequency f in the frequency domain.

In the following, *standard* deviates will be used. For example, if a_i has a normal distribution with variance $\sigma_{a_i}^2$, then the standard normal deviate $\xi_i=a_i/\sigma_{a_i}$ will be used. Similarly, if a_i has a uniform distribution over interval $[\min(a_i),\max(a_i)]$, then the standard uniform deviate $\xi_i=2\left(\frac{a_i-\min(a_i)}{\max(a_i)-\min(a_i)}-\frac{1}{2}\right)$ that is defined over $[-1,1]$, will be used. In both cases, the response of the uncertain system, $\mathbf{x}(t)$, depends on $\boldsymbol{\Xi}=(\xi_1,\ldots,\xi_r)$.

2.2. Fuzzy variables

Fuzzy variables are used when the information on the uncertain parameters is given in terms of intervals that reflect the possible values of these parameters [5]. Fuzzy variables are related to fuzzy sets $\overline{\mathcal{F}}$, defined by a set $\mathcal{F}$ and its membership function, $\mu_{\mathcal{F}}$, defined as

$$\begin{aligned}\mu_{\mathcal{F}}&: E\to[0,1]\\ &x\mapsto\mu_{\mathcal{F}}(x)\end{aligned}$$

where E is the set of definition of the fuzzy variable and $\mathcal{F}\subset E$. The concept of fuzzy sets was introduced by Zadeh [1] who interpreted the membership function as the degree of possibility for a variable to belong to $\mathcal{F}$ (i.e. the degree of membership of x in $\mathcal{F}$). If $\mu_{\mathcal{F}}(x)=0$ then x does not belong to $\mathcal{F}$, whereas $\mu_{\mathcal{F}}(x)=1$ indicates that x belongs to $\mathcal{F}$. When $0<\mu_{\mathcal{F}}(x)<1$ then

it is possible that x belongs to $\mathcal{F}$ and the degree of membership varies from weak to strong as $\mu_{\mathcal{F}}(x)$ varies from 0 to 1. The support of $\overline{\mathcal{F}}$ is

$$\mathrm{supp}(\overline{\mathcal{F}}) = \{x \in E | \mu_{\mathcal{F}}(x) > 0\}$$

An α-cut is defined by

$$\mathcal{F}_\alpha = \{x \in E | \mu_{\mathcal{F}}(x) \geq \alpha\} \quad \text{for } 0 < \alpha \leq 1$$

The element of $\mathcal{F}_\alpha$ has a degree of membership greater or equal to α.

In a fuzzy uncertainty propagation context, the objective is to provide the interval I_α whose bounds correspond to the minimum and the maximum of the response for all the α-cuts. So, for each α-cut and for each time t, the extrema of the solution of Eq. (1) must be calculated over all values that belong to the α-cut of the fuzzy variables. If the study is not in the time domain but in the frequency domain, then the frequency f would play the role of time t.

In the context of Eq. (2), $a_i^{(\alpha)}$ is an uncertain variable whose values are within an interval $\mathbf{a}_i^{(\alpha)}$. $\mathbf{A}_i^{(\alpha)}$ is the matrix associated with fuzzy variable a_i, for a given α-cut. Interval $\mathbf{a}_i^{(\alpha)}$ is defined as $\mathbf{a}_i^{(\alpha)} = [a_i^{(\alpha)m}, a_i^{(\alpha)M}]$, where $a_i^{(\alpha)m}$ and $a_i^{(\alpha)M}$ are the minimum and maximum of $a_i^{(\alpha)}$, respectively. For simplicity, a *standard* fuzzy variable ξ_i will be introduced by transforming $\mathbf{a}_i^{(\alpha)}$ to the interval $[-1, 1]$ by

$$\xi_i : \left[a_i^{(\alpha)m}, a_i^{(\alpha)M}\right] \to [-1, 1]$$
$$a_i^{(\alpha)} \mapsto \xi_i\left(a_i^{(\alpha)}\right) = 2\left(\frac{a_i^{(\alpha)} - a_i^{(\alpha)m}}{a_i^{(\alpha)M} - a_i^{(\alpha)m}} - \frac{1}{2}\right)$$

The inverse transformation is easily obtained as

$$a_i^{(\alpha)} : [-1, 1] \to \left[a_i^{(\alpha)m}, a_i^{(\alpha)M}\right]$$
$$\xi_i \mapsto a_i^{(\alpha)}(\xi_i) = \left(\frac{a_i^{(\alpha)M} - a_i^{(\alpha)m}}{2}\right)\xi_i + \left(\frac{a_i^{(\alpha)M} + a_i^{(\alpha)m}}{2}\right)$$

Then $\mathbf{x}^{(\alpha)}(t)$, the response of the uncertain system associated with a given α-cut depends on $\Xi = (\xi_1, \ldots, \xi_r) \in [-1, 1]^r$.

In the following, the membership function is supposed to be linear between $(a_i^{(0)m}, 0)$ and $(a_{i\ crisp}, 1)$, and between $(a_{i\ crisp}, 1)$ and $(a_i^{(0)M}, 0)$, as indicated in Fig. 1. Also, all of the uncertain matrices are assumed to be associated with a given α-cut, and so each matrix $\mathbf{A}$ should be denoted $\mathbf{A}^{(\alpha)}$. For simplicity, the superscript (α) will be dropped when it is not necessary.

3. Uncertain response

3.1. PC-components

The uncertain matrices are written as

$$\mathbf{M} = \mathbf{M}(\Xi) = \sum_{i=0}^{r} \xi_i \mathbf{M}_i \tag{3}$$

$$\mathbf{D} = \mathbf{D}(\Xi) = \sum_{i=0}^{r} \xi_i \mathbf{D}_i \tag{4}$$

$$\mathbf{K} = \mathbf{K}(\Xi) = \sum_{i=0}^{r} \xi_i \mathbf{K}_i \tag{5}$$

where $\xi_0 = 1$ is not an uncertain variable. Note that this definition implies that each uncertain parameter affects all of the

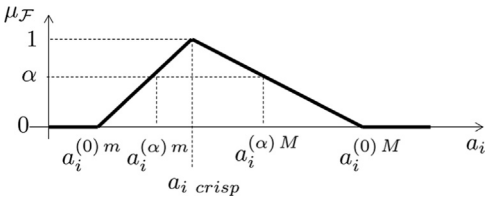

Fig. 1. A typical membership function.

mass, damping and stiffness matrices; usually each parameter will affect only one structural matrix, and in this case the ith terms for the other matrices will be zero.

Whatever the kind of uncertainty, the uncertain response vector is expanded in terms of polynomials Ψ_J, that are r-dimensional generalized polynomial chaoses, as

$$\mathbf{x}(t) = \sum_{J=0}^{+\infty} \mathbf{Y}_J(t)\Psi_J(\Xi) \tag{6}$$

where $\{\mathbf{Y}_J(t)\}$ are the PC-components of $\mathbf{x}(t)$. This expansion is common for random responses, but not for the case of fuzzy variables. The choice of the PC will be given in the following for each kind of uncertainty.

An approximation is obtained by truncating the infinite series as

$$\mathbf{x}^{\mathbf{P}}(t) = \sum_{J=0}^{P} \mathbf{Y}_J(t)\Psi_J(\Xi) \tag{7}$$

t will be dropped to shorten the equations. The multivariate polynomial chaoses used here are based on single variate polynomial chaoses $\psi_j(\xi_i)$ of order j. It is possible to define a bijection *Ind*:

$$\begin{aligned} &Ind\colon \mathbb{N} \to \mathbb{N}^r \\ &\quad J \mapsto (J_1, \ldots, J_r) \end{aligned}$$

such that

$$\Psi_J(\Xi) = \prod_{j=1}^{r} \psi_{J_j}(\xi_j) \tag{8}$$

where $m_J = \sum_{j=1}^{r} J_j$ is the order of Ψ_J. In Appendix A, *Ind* is defined for $r=2$.

By substituting $\mathbf{x}$ defined by expression (7) into Eq. (1), one has

$$\sum_{J=0}^{P} \Psi_J(\Xi)\left(\mathbf{M}\ddot{\mathbf{Y}}_J + \mathbf{D}\dot{\mathbf{Y}}_J + \mathbf{K}\mathbf{Y}_J\right) = \mathbf{F} \tag{9}$$

By using Eqs. (3)–(5),

$$\sum_{J=0}^{P}\sum_{k=0}^{r} \langle k,I,J\rangle\left(\mathbf{M}_k\ddot{\mathbf{Y}}_J + \mathbf{D}_k\dot{\mathbf{Y}}_J + \mathbf{K}_k\mathbf{Y}_J\right) = \delta_{0I}\mathbf{F}, \quad \text{for } I = 0, \ldots, P, \tag{10}$$

where δ_{IJ} is the Kronecker delta and

$$\langle k,I,J\rangle = \int_{\mathcal{D}_{\xi_1}} \cdots \int_{\mathcal{D}_{\xi_r}} \xi_k \Psi_I(\Xi)\Psi_J(\Xi)\, \mathrm{d}\Xi \tag{11}$$

with $\mathrm{d}\Xi = \prod_{j=1}^{r} p(\xi_j)\,\mathrm{d}\xi_j$ (examples of $p(\xi_j)$ are given in Appendix B) and $\mathcal{D}_{\xi_i}$ is the support of ξ_i.

Due to the polynomial chaos properties, quantities $\langle k,I,J\rangle$ may be easily derived (see Appendix B).

Define

$$\mathbf{C}_k \in \mathbb{R}^{(P+1)\times(P+1)}, \quad \text{with } [C_k]_{IJ} = \langle k,I,J\rangle \tag{12}$$

$$\tilde{\mathbf{M}} = \sum_{k=0}^{r} \mathbf{C}_k \otimes \mathbf{M}_k \in \mathbb{R}^{2(P+1)\times 2(P+1)} \tag{13}$$

$$\tilde{\mathbf{D}} = \sum_{k=0}^{r} \mathbf{C}_k \otimes \mathbf{D}_k \in \mathbb{R}^{2(P+1)\times 2(P+1)} \tag{14}$$

$$\tilde{\mathbf{K}} = \sum_{k=0}^{r} \mathbf{C}_k \otimes \mathbf{K}_k \in \mathbb{R}^{2(P+1)\times 2(P+1)} \tag{15}$$

$$\mathbf{Y} = [\mathbf{Y}_0^T\mathbf{Y}_1^T\cdots\mathbf{Y}_P^T]^T \in \mathbb{R}^{2(P+1)} \tag{16}$$

$$\tilde{\mathbf{F}}(t) = [\mathbf{F}^T(t)00\cdots0]^T \in \mathbb{R}^{2(P+1)} \tag{17}$$

where $\otimes$ denotes the Kronecker product and $(\bullet)^T$ denotes the transpose of $(\bullet)$. Then the components of the PC expansion satisfy

$$\tilde{\mathbf{M}}\ddot{\mathbf{Y}}(t) + \tilde{\mathbf{D}}\dot{\mathbf{Y}}(t) + \tilde{\mathbf{K}}\mathbf{Y}(t) = \tilde{\mathbf{F}}(t) \tag{18}$$

Hence, the PC-components are the solution of a $2(P+1)$ degrees of freedom (dofs) dynamical system that will be referred to the PC-system. Accordingly the PCE transforms the study of an uncertain dynamical system to the study of a deterministic dynamical system. Accordingly the PC-system has resonant frequencies and the random/fuzzy steady-state response characteristics to a harmonic force will show peaks related to these spurious resonances: the latter will be referred to as PC-resonances.

3.2. Random variables

The choice of the polynomial chaos depends on the distribution of the random variable: Hermite polynomials are used for normal distribution whereas Legendre polynomial are used for uniform distribution. They are an orthogonal basis over the probability measure of the random variable. The PC technique can deal with different kinds of random variables. Thus, for example, if one uncertainty is modeled by a normal variate, ξ_1 and another one by a uniform variable, ξ_2, then the polynomial chaos $\Psi_J(\xi_1,\xi_2)$ is a product of a Hermite polynomial $H_{J_1}(\xi_1)$ by a Legendre polynomial $L_{J_2}(\xi_2)$. Although the Hermite polynomials are not orthogonal to the Legendre polynomials, this is not necessary because we assume ξ_1 and ξ_2 are independent random variables.

As the behavior of Hermite polynomials was studied in previous papers [20,21], they will not be discussed further in this work.

3.3. Fuzzy variables

Legendre polynomials L_i are defined over the interval $[-1,1]$ that is the support of each standard fuzzy variable ξ_k and are orthogonal with respect to the inner product:

$$\int_{-1}^{1} L_i(\xi)L_j(\xi)\,\mathrm{d}\xi = \frac{2}{2i+1}\delta_{ij} \tag{19}$$

Hence the Legendre polynomials are perfectly adapted to describe the propagation of the uncertainty related to the standard fuzzy variables.

3.4. Uncertainty propagation

Once the coefficients $\mathbb{Y}$ are calculated, the uncertain response is evaluated using Eq. (7). If the response is a random variable, the characteristics may be determined by a Monte Carlo simulation (MCS), which is direct and very fast. Further the mean value is given directly by $\mathbf{Y}_0$, the first coefficient of the expansion, and the standard deviation of dof x_i is estimated as

$$\sigma^2_{x_i(t)} = \sum_{J=1}^{P} \langle 0,J,J\rangle \left(\{\mathbf{Y}_J\}_i(t)\right)^2 \tag{20}$$

If the response is fuzzy, then the extrema must be determined for each α-cut and for each time t (or for each frequency ω if a frequency response is calculated). In general this is an optimization problem, however here we take a direct approach by evaluating the response directly using the PCE (Eq. (7)) for n parameter values $\{\Xi_i\}_{i=1\ldots n}$ that discretize the α-cut; the minimum and the maximum of the response then give the interval of the response. Obviously n must be sufficient to obtain the extrema with good accuracy.

3.5. Mixed uncertain variables

As the formalism is exactly the same, whatever the form of the uncertainty, it is possible to deal with mixed (fuzzy and random) uncertain variables directly. In this case the PCs that describe the fuzzy variables are Legendre polynomials, whereas the PCs that describe the random variables depend on the associated probability distribution.

However, the problem of describing the uncertain response remains. Indeed the uncertain response is both random and fuzzy. Here we assume that the mean response and the standard deviation are given as fuzzy variables.

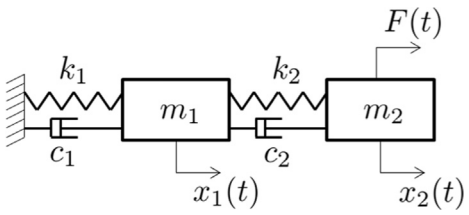

Fig. 2. The two degrees-of-freedom system with stochastic stiffness coefficients.

Table 1
The characteristics of the discrete system.

m (kg)	c ($\mathrm{Nm^{-1}\,s^{-1}}$)	$k_{1,\mathrm{crisp}}$ ($\mathrm{kNm^{-1}}$)	$k_{2,\mathrm{crisp}}$ ($\mathrm{kNm^{-1}}$)	δ_{k1} (%)	δ_{k2} (%)	F_0 (N)
1	1	15	15	5	5	1

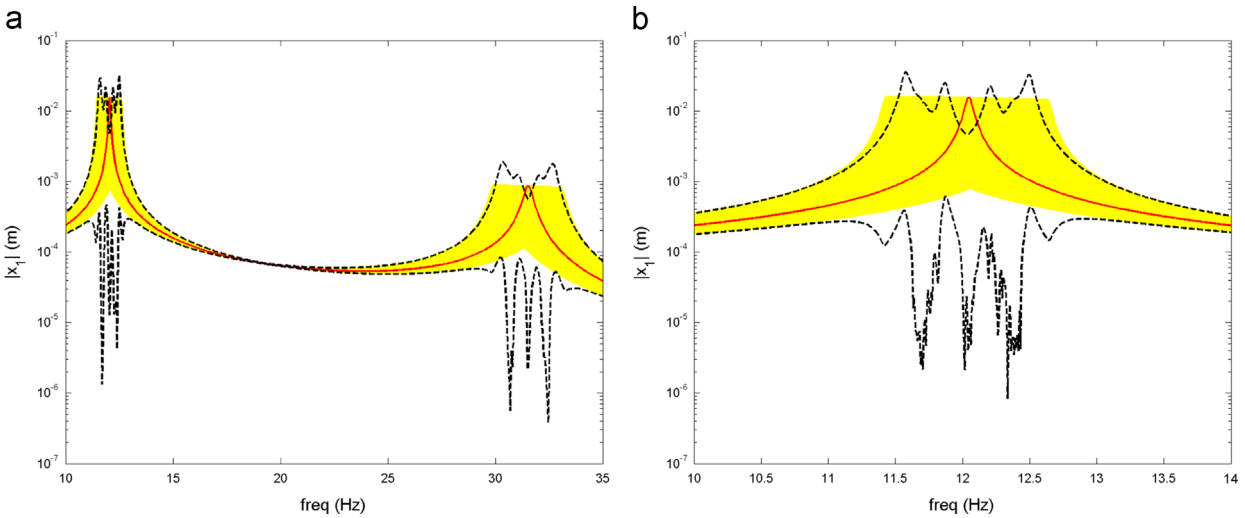

Fig. 3. The discrete system with two uncertain fuzzy stiffnesses: (a) both modes, (b) zoom around the first deterministic eigenfrequency. Solid line: crisp response; Dashed line: PC interval response using Legendre polynomials of order 3; Shadow area: direct interval response.

4. Examples

4.1. Discrete system with two uncertain parameters

The discrete two dof system is shown in Fig. 2. In this example, the stiffnesses k_1 and k_2 are assumed to be uncertain and independent. Table 1 gives the characteristics of the uncertain system. In this example the random and fuzzy models of the uncertain stiffnesses will be applied separately. The pdfs of the random stiffnesses are assumed to be uniform with

$$\min(k_i) = (1-\delta_{ki})k_{i,\mathrm{crisp}}, \quad \max(k_i) = (1+\delta_{ki})k_{i,\mathrm{crisp}} \ \text{ for } i = 1,2$$

The fuzzy variables at the zero α-cut are given by

$$k_i^{(0)m} = (1-\delta_{ki})k_{i,\mathrm{crisp}}, \quad k_i^{(0)M} = (1+\delta_{ki})k_{i,\mathrm{crisp}} \ \text{ for } i = 1,2$$

The second mass is excited by a sinusoidal force of amplitude F_0, and the output of interest is the displacement of the first mass in the frequency domain.

Fig. 3 gives the frequency response function interval for the zero α-cut of the fuzzy system. For comparison, Fig. 4 gives the mean and standard deviation for the uniform random stiffness case. In each figure, the results are calculated with the PC approach (PC of order 3) and with a direct approach (Monte Carlo simulation for the random system using Latin hypercube sampling). Spurious oscillations are shown in all of the figures when the results are derived with the PC approach, due to the PC eigen-frequencies, as already mentioned in Section 3.1. However, by comparison with the results presented in previous papers [20,21], the amplitude of these oscillations is much larger when Hermite polynomials are used as opposed to Legendre polynomials.

To study the influence of the PC order, the same simulations were performed for PC orders of 20 and 50. Figs. 5 and 6 show the results for the fuzzy stiffness uncertainty. The upper bound of the response interval is well estimated with the increase of the PC order whereas the lower bound is not really improved. From an engineering point of view, the upper bound is most important and for this case the PC simulation approximates the upper accurately. Fig. 7 shows the results for the uniform random stiffness uncertainty. The results are provided around the deterministic first eigenfrequency where the PC convergence is slower so as to highlight the behavior of the PC response. The convergence is fast when increasing the PC order of the Legendre polynomials whereas previous papers [20,21] showed a slow convergence with Hermite polynomials for Gaussian random variables.

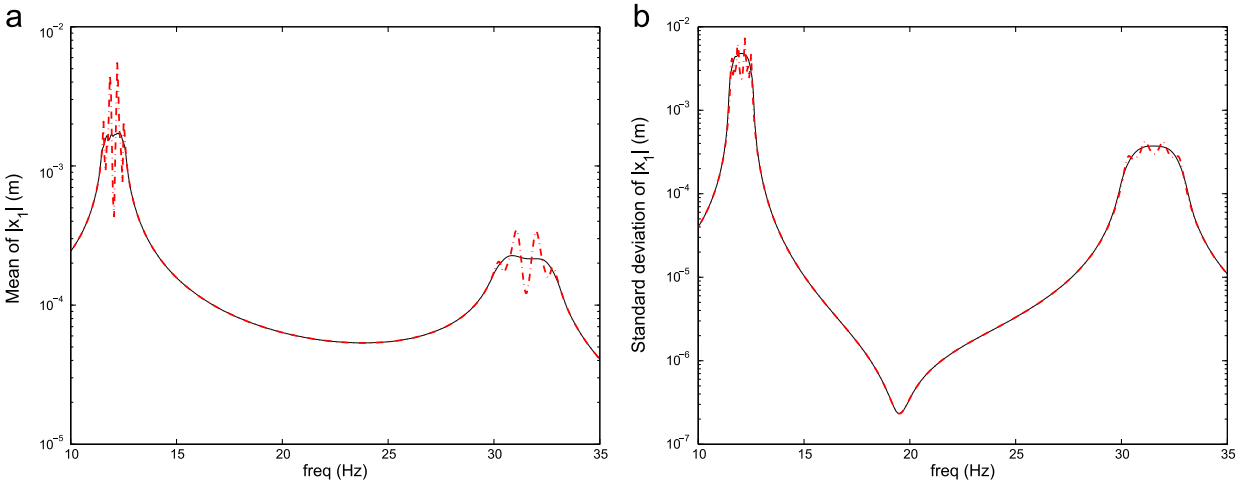

Fig. 4. The discrete system with two uncertain random stiffnesses: (a) mean, (b) standard deviation. Solid line: MC simulation; Dashed line: PC using Legendre polynomials of order 3.

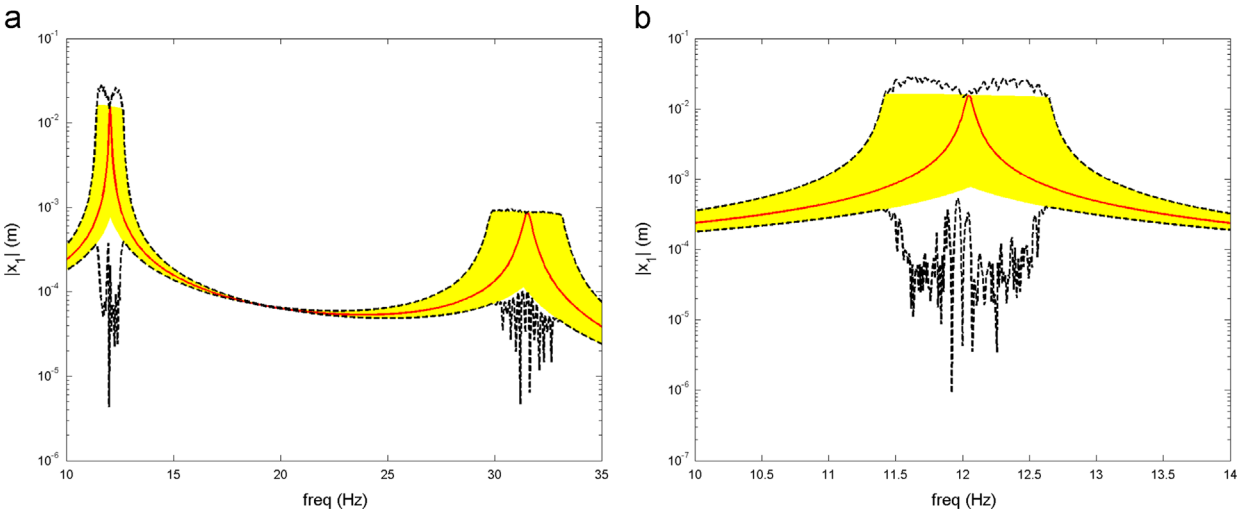

Fig. 5. The discrete system with two uncertain fuzzy stiffnesses: (a) both modes, (b) zoom around the first deterministic eigenfrequency. Solid line: crisp response; Dashed line: PC interval response using Legendre polynomials of order 20; Shadow area: direct interval response.

4.2. Beam with mixed uncertainties

The pinned–pinned beam system is shown in Fig. 8. The beam is modeled with three nodes and two Euler-Bernoulli beam elements, resulting in four degrees of freedom. In this example, the flexural rigidity, EI, where E is the Young's modulus and I the cross-section inertia, and the damping ratio, ζ, are assumed to be uncertain. In contrast to the previous example, the nature of the uncertainties is not the same for both parameters; EI is assumed to be a uniform random variable whereas ζ is assumed to be a fuzzy variable, such that the 0-cut is the interval [0.055]% and the crisp value is 0.5%. As a consequence, the mass matrix $\mathbf{M}$ is deterministic, and the stiffness matrix $\mathbf{K}$ is random and is defined by Eq. (5): the mean of $\mathbf{K}$ is then $\mathbf{K}_0$. The characteristics of beam system and the random parameter are listed in Table 2. The beam is excited at its left end by a sinusoidal moment $C(t)$ of amplitude C_0, and the output of interest is the rotation of the left end of the beam in the frequency domain.

The damping ratio is assumed to be the same for each mode, and the damping matrix is defined as

$$\mathbf{D} = 2\zeta\mathbf{M}\left[\mathbf{M}^{-1}\mathbf{K}_0\right]^{1/2} \tag{21}$$

The response interval of the mean and the standard deviation of the mixed uncertain system is given in Fig. 9 for a PCE order equal to 3. In each figure, the results are calculated with the PC approach (PC of order 3) and with a direct approach (Monte Carlo simulations for the random system). In practice the 0-cut interval is divided in 100 sub-intervals, and for each of the 101 values for damping ζ an MCS using Latin hypercube sampling (2000 samples) was performed to estimate the first

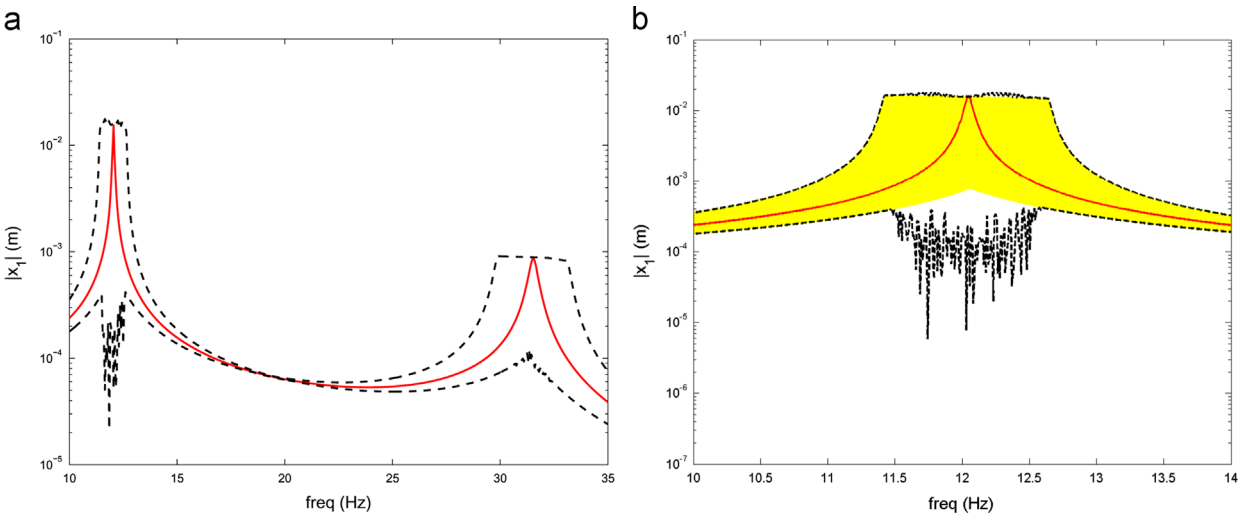

Fig. 6. The discrete system with two uncertain fuzzy stiffnesses: (a) both modes, (b) zoom around the first deterministic eigenfrequency. Solid line: crisp response; Dashed line: PC interval response using Legendre polynomials of order 50; Shadow area: direct interval response.

two moments. Then the minimum and the maximum values of these moments were determined over the 0-cut interval. This procedure was used for both the MCS and the PCE.

As expected, around the crisp or deterministic eigenfrequencies the PCE has not converged whereas the results are in an excellent agreement with the MCS results elsewhere. To improve the results, the PC order was increased to 10 and 20, and the results are given in Figs. 10 and 11, respectively. A PC order of 10 provided good results for the estimation of the mean whereas a PC order equal to 20 provided excellent results. However, surprisingly, the results are not as good for the standard deviation: that means the probability density function is probably not very well estimated. So, in this case study, the PCE has not converged sufficiently with a PC order equal to 20 to obtain a good estimate for the higher order statistical moments.

This approach allows the response to be calculated for the membership function of the damping given in Fig. 12. Fig. 13 shows the fuzzy response of the mean and the standard deviation when the frequency is equal to the first deterministic eigenfrequency. In particular, the fuzzy response is not linear with respect to α; the evolution of the mean is even not monotonic between the minimum value of the 0-cut, $(\zeta^{(0)m}, 0)$, and the crisp value, $(\zeta_{crisp}, 1)$ (Fig. 13(a)). This is a consequence of the strong asymmetry in the membership function, that is when the mid-0-cut value is far from the crisp value. Indeed, it has been verified that if the crisp value is increased to 0.7%, then the evolution becomes monotonic.

4.3. Rotor example

The last example describes the response of an uncertain two-bearing flexible rotor to out-of-balance forces (as illustrated in Fig. 14). The system consists of a shaft (length L, diameter d_s, density ρ_s, Young's modulus E_s) carrying a rigid circular disk (density ρ_d, inside diameter d_i, outside diameter d_o, thickness h). The bearings are elastically supported in both horizontal and vertical directions at the ends of the shaft; the stiffness may be different in the vertical and horizontal directions and are given by k_{ix} and k_{iy} for the i-th bearing (bearing 1 is at the left end, and bearing 2 at the right end of the shaft). The machine is excited by an out-of-balance force on the disk. This unbalance force is represented by an additional mass m at a distance e from the center of rotation of the shaft (i.e. e defines the eccentricity of the mass).

4.3.1. System model

The shaft is modeled by 8 beam elements which include the shear and rotary inertia effects. There are 4 degrees of freedom (dof) per node (i.e. the horizontal and vertical displacements and the two associated rotations), which gives a total of 36 dofs. The axial and torsional degrees of freedom are not considered here. The equations of motion of the rotor system can be written as

$$\mathbf{M}\ddot{\mathbf{x}}(t)+(\mathbf{C}+\omega\mathbf{G})\dot{\mathbf{x}}(t)+\mathbf{K}\mathbf{x}(t)=\mathbf{F}(t) \tag{22}$$

The mass matrix **M** includes the inertia properties of both the shaft and the rigid disk. The matrices **C** and **G** represent the effects of the shaft internal damping and gyroscopic moments for both the shaft and the disk. The matrix **K** includes the stiffness matrices of the shaft and the supports. **F** defines the out-of-balance forces for the rotor system. Friswell et al. [22] give further details of the modeling of rotating machines used here.

Table 3 gives the values of the deterministic physical parameters of the rotor. The Campbell diagram of this machine is shown in Fig. 15 and highlights that the first and second backward and forward critical speeds (at 34.7, 41.4, 116.6 and 127.7 Hz) are in the rotor speed range of interest.

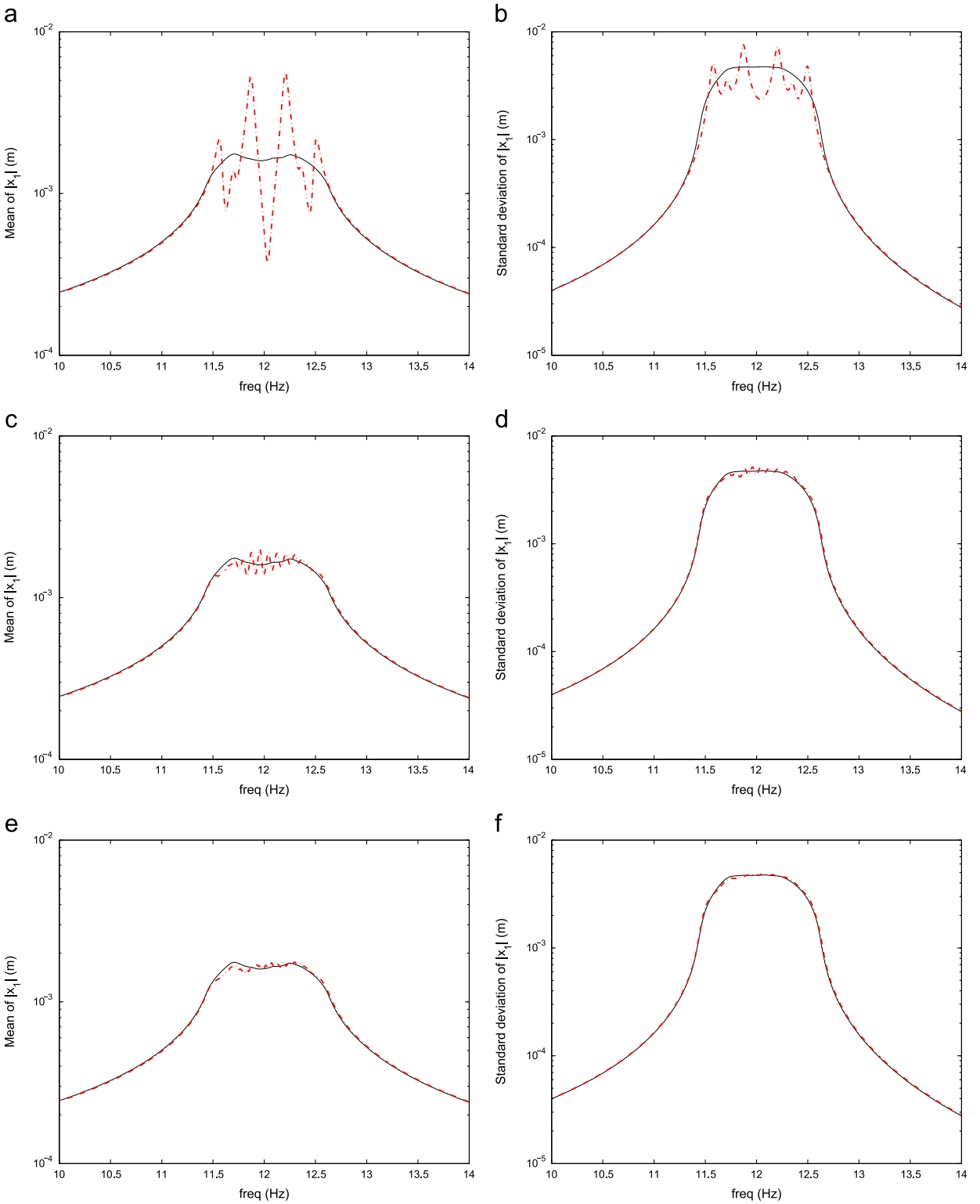

Fig. 7. The discrete system with two uncertain random stiffnesses: (a) mean for PC order 3, (b) standard deviation for PC order 3, (c) mean for PC order 20, (d) standard deviation for PC order 20, (e) mean for PC order 50, (f) standard deviation for PC order 50. Solid line: MC simulation; Dashed line: PC using Legendre polynomials.

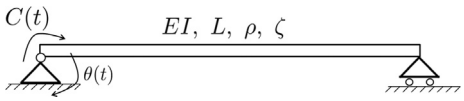

Fig. 8. Schematic of the uncertain beam.

Table 2
Beam characteristics and uncertain parameters.

L (m)	ρA (kg/m)	C_0 (kN)	min(EI) (kNm^2)	max(EI) (kNm^2)
1	7800	1	90	125
ζ_{crisp} (%)	$\zeta^{(0)m}$ (%)	$\zeta^{(0)M}$ (%)		
0.5	0.05	5		

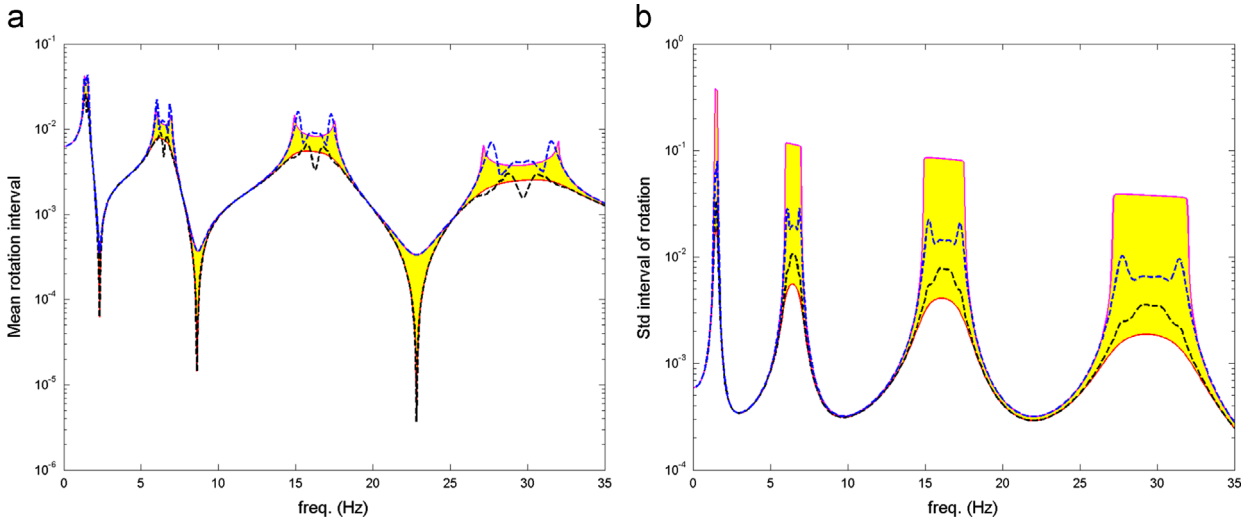

Fig. 9. The response of the beam example with random EI and fuzzy ζ using Legendre polynomials of order 3: (a) mean, (b) standard deviation. Solid line: MC simulation; Dashed line: PC using Legendre polynomials.

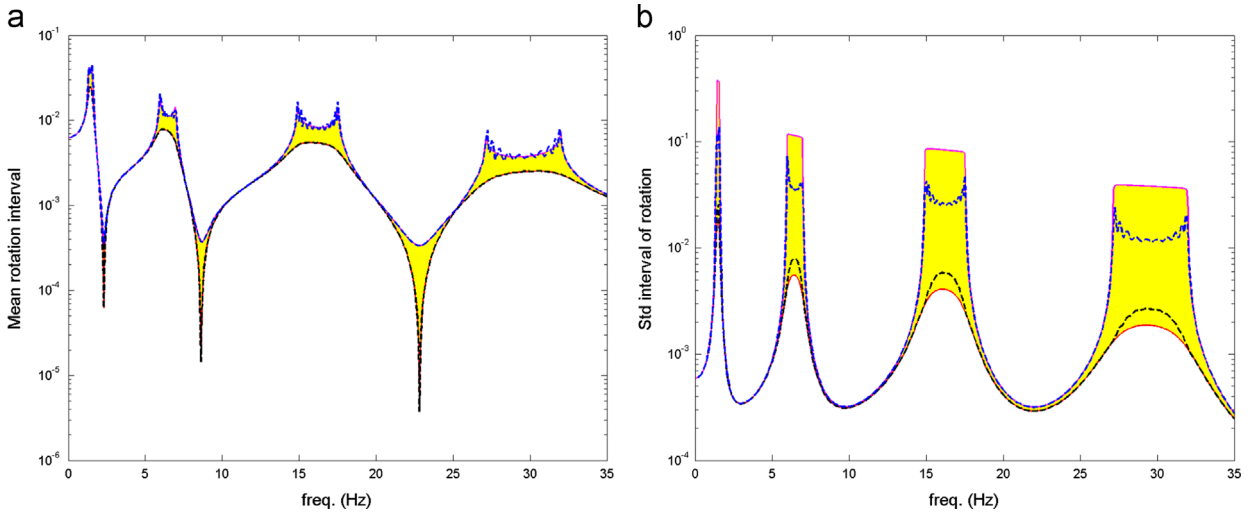

Fig. 10. The response of the beam example with random EI and fuzzy ζ using Legendre polynomials of order 10: (a) mean, (b) standard deviation. Solid line: MC simulation; Dashed line: PC using Legendre polynomials.

4.3.2. Uncertainties in the rotor system

In practice, several parameters may be uncertain. In the following, the shaft Young's modulus, E_s, the horizontal spring stiffness of bearing 1, k_{1x}, and, disk thickness, h, are assumed to be uncertain parameters. The stiffness matrix is a linear

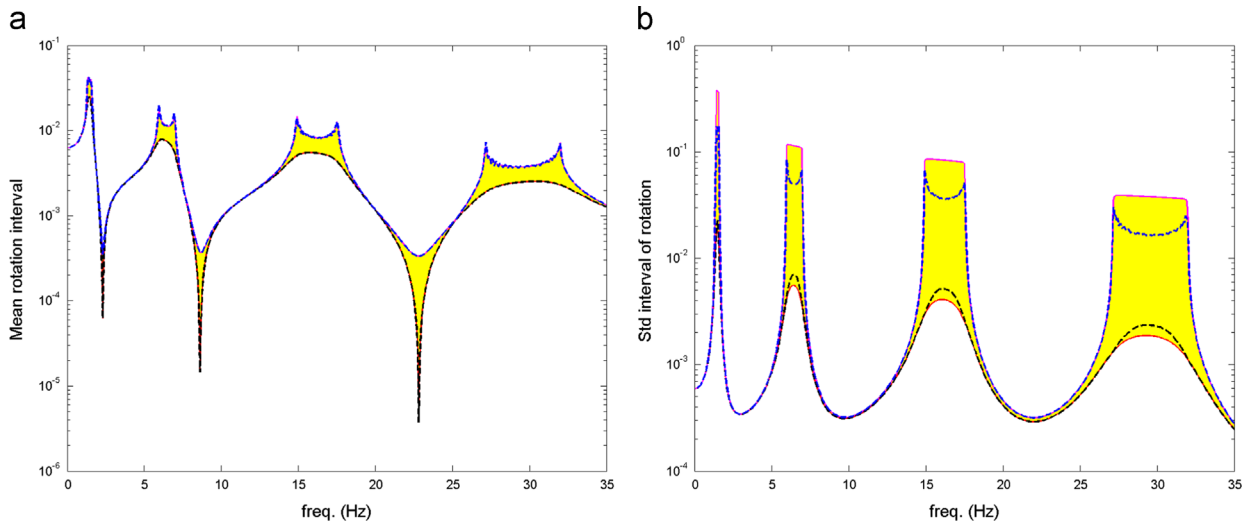

Fig. 11. The response of the beam example with random *EI* and fuzzy ζ using Legendre polynomials of order 20: (a) mean, (b) standard deviation. Solid line: MC simulation; Dashed line: PC using Legendre polynomials.

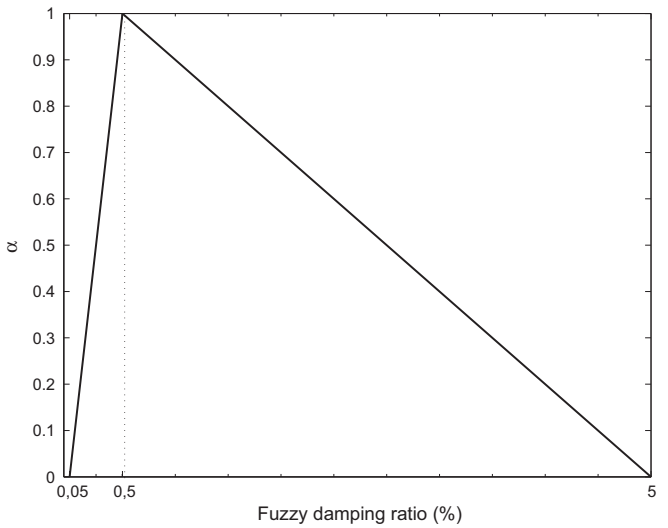

Fig. 12. Membership function of the damping ratio.

function of E_s and k_{1x}, and both the mass and gyroscopic matrices are linear functions of h. The other parameters keep their deterministic stiffness values.

The damping matrix is assumed to be deterministic and proportional to the mass and stiffness matrices at the mean or crisp values of the random or fuzzy parameters. Of course other models of the damping, including uncertainty, may be considered.

Two cases will be considered and are listed in Table 4. In case 1, E_s is a uniform random variable and k_{1x} is a fuzzy variable. In case 2, E_s is a uniform random variable and h is a fuzzy variable. E_s follows a uniform distribution with $\min(E_s) = E_{s0} - \Delta E_s$ and $\max(E_s) = E_{s0} + \Delta E_s$.

The uncertain vertical and horizontal displacements, v and u, located at node 4, 0.3 m from the left end of the shaft, will be the response quantities of interest (see Fig. 14).

4.3.3. Case 1: random E_s and fuzzy k_{1x}

In this case, the thickness of the disk, h, is assumed to be deterministic and equal to h_0. The two uncertain parameters are the Young's modulus of the shaft, E_s, and the horizontal stiffness of bearing 1. The Young modulus is assumed to be a random parameter with a uniform distribution and the horizontal support stiffness is assumed to be a fuzzy parameter.

Fig. 16 shows the intervals for the mean and standard deviation for vertical displacement at node 4. Fig. 17(a) shows the corresponding results for the horizontal displacement. A PCE order equal to 20 is chosen. Since the horizontal stiffness of

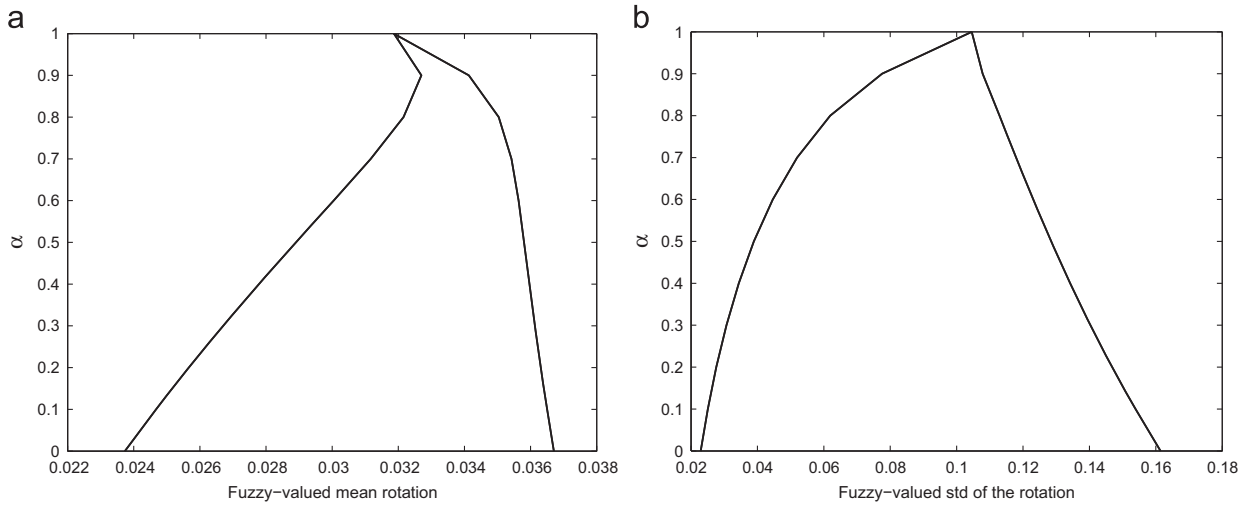

Fig. 13. Fuzzy response at the first deterministic eigenfrequency for a PC order of 20: (a) Mean, (b) standard deviation.

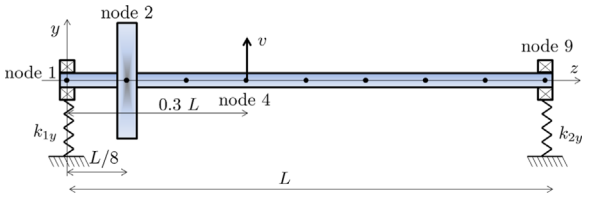

Fig. 14. The two bearing flexible rotor.

Table 3
Characteristics of the deterministic rotor system. The 0 indicates the value of an uncertain parameter used when a deterministic quantity is required.

Shaft		Disk		Support		Force	
E_{s0}	210 GPa	ρ_d	7800 kg m^{-3}	k_{1x0}	3 MN m^{-1}	$m \times e$	10^{-4} kg m
L	1 m	h_0	3 cm	k_{1y}	3 MN m^{-1}		
ρ_s	7800 kg m^{-3}	d_{inner}	2 cm	k_{2x}	3 MN m^{-1}		
d_s	2 cm	d_{outer}	20 cm	k_{2y}	3 MN m^{-1}		

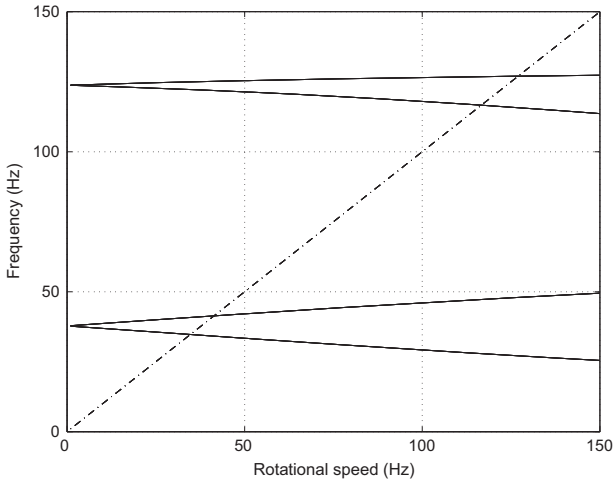

Fig. 15. The Campbell diagram of the flexible rotor.

Table 4
Uncertain parameters of the rotor system.

Case 1	E_s k_{1x}	Mean(E_s) $k_{1x,\mathrm{crisp}}$	E_{s0} k_{1x0}	ΔE_s k_{1x}^m	5% E_{s0} 2.5 MN m^{-1}	k_{1x}^M	3.5 MN m^{-1}
Case 2	E_s h	Mean(E_s) h_{crisp}	E_{s0} h_0	ΔE_s h^m	5% E_{s0} 2.5 cm	h^M	3.5 cm

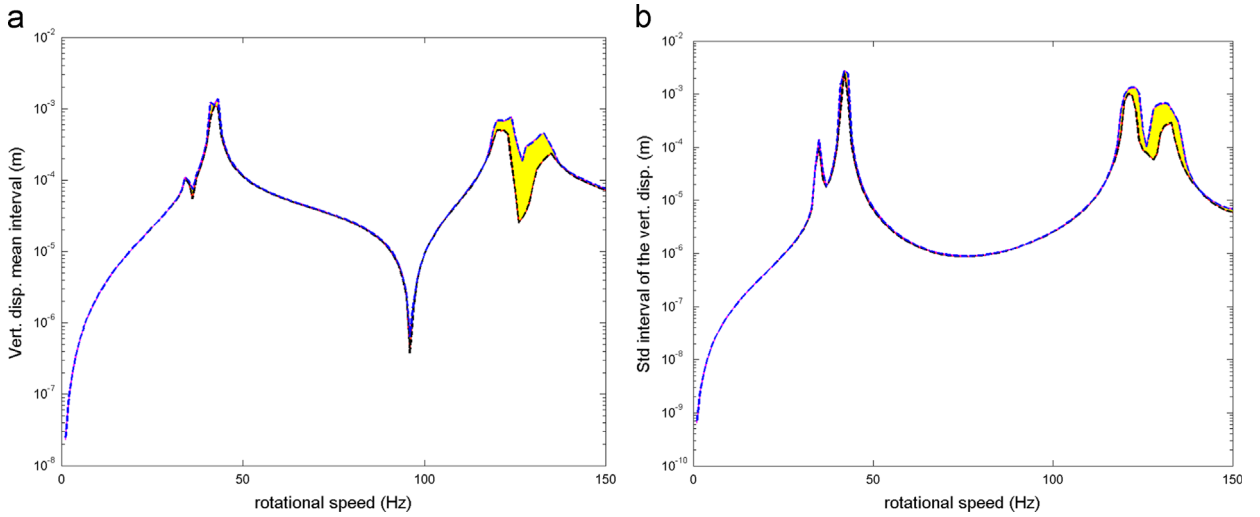

Fig. 16. Vertical displacement for the rotor system with random E_s and fuzzy k_{1x} using Legendre polynomials of order 20: (a) mean, (b) standard deviation. Solid line: MC simulation; Dashed line: PC response.

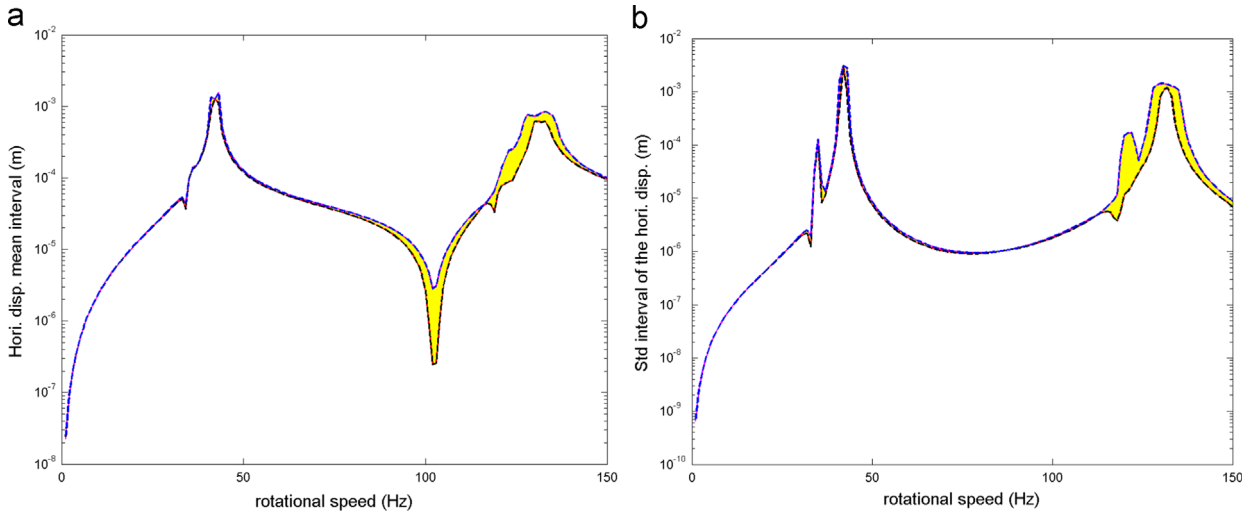

Fig. 17. Horizontal displacement for the rotor system with random E_s and fuzzy k_{1x} using Legendre polynomials of order 20: (a) mean, (b) standard deviation. Solid line: MC simulation; Dashed line: PC response.

one bearing is now a fuzzy parameter, the support stiffness is anisotropic and responses at the first and second backward critical speeds appear. The stiffness uncertainties also naturally introduce an increase or decrease all critical speeds and the associated amplitudes levels.

The proposed approach allows the response to be predicted for the frequency range of interest and more specifically around the backward and forward critical speeds: the PCE results are in an excellent agreement with the MCS results.

4.3.4. Case 2: random E_s and fuzzy h

The effects of uncertainties in the Young modulus of the shaft E_s and the thickness of the disk h are now studied. The horizontal stiffness of bearing 1 is assumed to be deterministic and equal to k_{1x0}. The Young's modulus is chosen as a

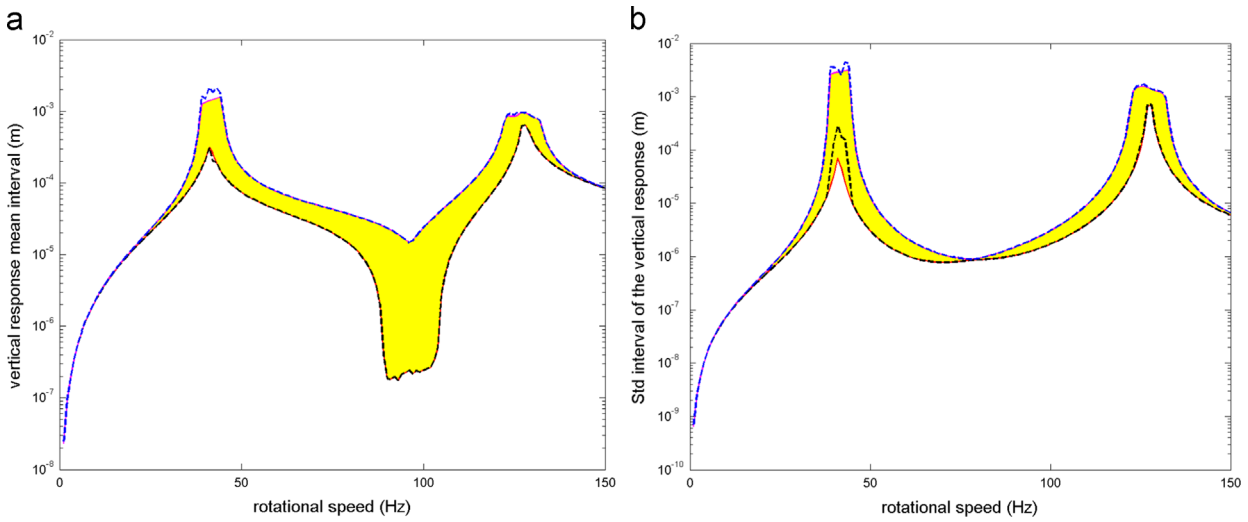

Fig. 18. Vertical displacement for the rotor system with random E_s and fuzzy h using Legendre polynomials of order 20: (a) mean, (b) standard deviation. Solid line: MC simulation; Dashed line: PC response.

random parameter with a uniform distribution and the thickness of the disk is chosen as a fuzzy parameter. The uncertainty in the thickness of the disk will generate two fuzzy matrices, i.e. the mass and gyroscopic matrices.

The response interval of the mean and the standard deviation of the mixed uncertain system is given in Fig. 18 for the vertical displacement and a PCE order equal to 20. The horizontal displacement is not plotted as it is identical to the vertical displacement as the support stiffness is now isotropic. The presence of parameter uncertainties generates significant variation in the dynamic response of the rotor. However, significant differences between this case and the previous study (see Section 4.3.3) are clearly observed. First of all, the first and second backward critical speed are not present since the support stiffness is now isotropic. Secondly, the variations of the two forward critical speeds in terms of frequency and amplitude level are much higher. This indicates that the variation of the disk thickness has a significant impact on the vibrational response of the rotor, which is easily explained by its contributions to the gyroscopic effects and the mass. Finally, a high variation of the anti-resonance position is also observed due to the uncertainty of the disk thickness. The PCE results are again validated by the Monte Carlo simulations.

5. Conclusion

The use of the polynomial chaos allow a unified processing of uncertainty; random variables and fuzzy variables lead to the same PC equations. The post-processing of the PC expansion depends on the nature of the uncertainty: an optimization problem is solved for the fuzzy variables whereas the statistical moments are derived for the random variables. The PC resonance issue already mentioned in [20] for random variables was also demonstrated for fuzzy variables. However, the fuzzy variables are associated with Legendre polynomials that exhibit faster convergence than Hermite polynomial. However, the main interest of the PCE is to provide a general framework to deal with mixed uncertainties. This paper demonstrated an approach that is able to efficiently propagate uncertainty modeled with both random and fuzzy parameters.

Acknowledgments

J.-J. Sinou acknowledges the support of the Institut Universitaire de France.

Appendix A. Decomposition of index I, for $r=2$

For a given index I, Ψ_I must be expanded as a product of two Legendre polynomials:

$$\Psi_I(\xi_1,\xi_2)=\psi_{I_1}(\xi_1)\psi_{I_2}(\xi_2) \tag{A.1}$$

and $m_I=I_1+I_2$ is the order of Ψ_I. The number of polynomials whose order is lower or equal to m is $\binom{m+2}{2}$. So, if m_I is the

Table A5
Index decomposition.

I	I_1	I_2	Order
1	1	0	1
2	0	1	1
3	2	0	2
4	1	1	2
5	0	2	2
6	3	0	3
7	2	1	3
8	1	2	3
9	0	3	3
10	4	0	4
11	3	1	4
12	2	2	4
13	1	3	4
14	0	4	4
15	5	0	5
16	4	1	5
17	3	2	5
18	2	3	5
19	1	4	5
20	0	5	5

order of Ψ_I, I satisfies

$$I \geq \binom{m+1}{2} = \frac{m_I(m_I+1)}{2} \tag{A.2}$$

$$I < \binom{m+2}{2} = \frac{(m_I+1)(m_I+2)}{2} \tag{A.3}$$

Then, as m_I is an integer, one can deduce

$$m_I = \left\lfloor \frac{\sqrt{8I+1}-1}{2} \right\rfloor \tag{A.4}$$

Consider indexes I and J. They are decomposed according to the rules:
1. If $I<J$ then order $(\Psi_I) \leq$ order(Ψ_J).
2. If $I<J$ and order $(\Psi_I) =$ order(Ψ_J) then $I_1 > J_1$ and $I_2 < J_2$.

Then I_2 and I_1 may be defined as

$$I_2 = I - \frac{m_I(m_I+1)}{2} \tag{A.5}$$

$$I_1 = m_I - I_2 \tag{A.6}$$

For indexes I_1, I_2 given, I is defined as

$$I = I_2 + \frac{(I_1+I_2)(I_1+I_2+1)}{2} \tag{A.7}$$

Eqs. (A.4) and (A.5)–(A.7) define the mapping *Ind*. The decomposition is given for I from 0 to 20 in Table A5.

These two rules may be easily extended for $r>2$ to define a general decomposition of index I.

Appendix B. Legendre polynomial chaos

Polynomial $\psi_i(\xi)$ is equal to the Legendre polynomial of order i, $L_i(\xi)$. Then

$$\Psi_J(\Xi) = \prod_{j=1}^{r} L_{J_j}(\xi_j) \tag{B.1}$$

where $m_J = \sum_{j=1}^{r} J_j$ is the order of Ψ_J. We have

$$\langle k, I, J\rangle = \int_{\xi_1=-1}^{1} \cdots \int_{\xi_r=-1}^{1} \xi_k \Psi_I(\Xi)\Psi_J(\Xi)\, \mathrm{d}\Xi \tag{B.2}$$

with $\mathrm{d}\Xi = \prod_{j=1}^{r} \mathrm{d}\xi_j$.

The properties of Legendre polynomials then give

$$\langle 0, I, J\rangle = \int_{\xi_1=-1}^{1} \cdots \int_{\xi_r=-1}^{1} \Psi_I(\Xi)\Psi_J(\Xi)\, \mathrm{d}\Xi = \prod_{i=1}^{r} \frac{2}{2J_i+1}\delta_{IJ} \tag{B.3}$$

and for $k \geq 1$

$$\begin{aligned}\langle k, I, J\rangle &= \int_{\xi_1=-1}^{1} \cdots \int_{\xi_r=-1}^{1} \xi_k \Psi_I(\Xi)\Psi_J(\Xi)\, \mathrm{d}\Xi = \int_{\xi_k=-1}^{1} \xi_k L_{J_k}(\xi_k) L_{I_k}(\xi_k)\, \mathrm{d}\xi_k \prod_{\substack{i=1\\ i\neq k}}^{r} \int_{\xi_i=-1}^{1} L_{J_i}(\xi_i) L_{I_i}(\xi_i)\, \mathrm{d}\xi_i \\ &= \left(\frac{J_k+1}{2J_k+3}\frac{2}{2J_k+1}\delta_{J_k+1,I_k} + \frac{J_k}{2J_k+1}\frac{2}{2J_k-1}\delta_{J_k-1,I_k}\right) \prod_{\substack{i=1\\ i\neq k}}^{r} \frac{2}{2J_i+1}\delta_{J_i,I_i}\end{aligned} \tag{B.4}$$

where I_i and J_i are the i-th elements of $Ind(I)$ and $Ind(J)$, respectively.

References

[1] L.A. Zadeh, Fuzzy sets, Inf. Control (1965) 338–353.
[2] D. Moens, D. Vandepitte, A survey of non-probabilistic uncertainty treatment in finite element analysis, Comput. Methods Appl. Mech. Eng. 194 (2005) 1527–1555.
[3] H. De Gersem, D. Moens, W. Desmet, D. Vandepitte, A fuzzy finite element procedure for the calculation of uncertain frequency response functions of damped structures: part 2, numerical case studies, J. Sound Vib. 288 (2005) 463–486.
[4] D. Moens, D. Vandepitte, A fuzzy finite element procedure for the calculation of uncertain frequency-response functions of damped structures: part 1, procedure, J. Sound Vib. 288 (2005) 431–462.
[5] M. Hanss, Applied Fuzzy Arithmetic: An Introduction with Engineering Applications, Springer, Berlin Heidelberg, 2010.
[6] S. Beer, M. Ferson, V. Kreinovich, Imprecise probabilities in engineering analyses, Mech. Syst. Signal Process. 37 (1–2) (2013) 4–29.
[7] R. Ghanen, D. Spanos, Stochastic Finite Elements: A Spectral Approach, Springer-Verlag, New York, USA, 1991.
[8] G.I. Schueller, H.J. Pradlwarter, Uncertainty analysis of complex structural systems, Int. J. Numer. Methods Eng. 80 (6–7, Sp. Iss. SI) (2009) 881–913.
[9] G. Stefanou, The stochastic finite element method: past, present and future, Comput. Methods Appl. Mech. Eng. 198 (2009) 1031–1051.
[10] B. Sudret, A. Der Kiureghian, Technical Report UCB/SEMM-2000/08, University of Berkeley, 2000.
[11] D. Xiu, G.E. Karniadakis, The Wiener-Askey polynomial chaos for stochastic differential equations, SIAM J. Sci. Comput. 24 (2) (2002) 614–644.
[12] D. Xiu, G.E. Karniadakis, Modeling uncertainty in flow simulations via generalized polynomial chaos, J. Comput. Phys. 187 (1) (2003) 137–167.
[13] G. Blatman, B. Sudret, Use of sparse polynomial chaos expansions in adaptive stochastic finite element analysis, Probab. Eng. Mech. 25 (2010) 183–197.
[14] G. Blatman, B. Sudret, Adaptive sparse polynomial chaos expansion based on least angle regression, J. Comput. Phys. 230 (2011) 2345–2367.
[15] S. Adhikari, A spectral projection approach for fuzzy uncertainty propagation in structural dynamics, in: Uncertainty in Structural Dynamics Conference – USD2012, Leuven, Belgium, 2012, pp. 4745–4759.
[16] S. Adhikari, H. Haddad Khodaparast, A spectral approach for fuzzy uncertainty propagation in finite element analysis, Fuzzy Sets Syst. 243 (2014) 1–24.
[17] A. Monti, F. Ponci, M. Valtorta, Extending polynomial chaos to include interval analysis, IEEE Trans. Instrum. Meas. 59 (1) (2010) 48–55.
[18] K. Sepahvand, S. Marburg, On construction of uncertain material parameter using generalized polynomial chaos expansion from experimental data, Proc. IUTAM 6 (2013) 4–17.
[19] K. Sepahvand, S. Marburg, Identification of composite uncertain material parameters from experimental modal data, Probab. Eng. Mech. 37 (2014) 148–153.
[20] E. Jacquelin, S. Adhikari, J.-J. Sinou, M.I. Friswell, The polynomial chaos expansion and the steady-state response of a class of random dynamic systems, J. Eng. Mech. 141 (4) (2015) 04014145.
[21] J.-J. Sinou, E. Jacquelin, Influence of polynomial chaos expansion order on uncertain rotor system response, Mech. Syst. Signal Process. 50–51 (2015) 718–731.
[22] M.I. Friswell, J.E.T. Penny, S.D. Garvey, A.W. Lees, Dynamics of Rotating Machines, Cambridge University Press, Cambridge, United Kingdom, 2010.